Preparative, X-ray, and NMR Studies of Phosphide-Bridged Palladium(I) Dimers. A New Complex with an η^2-Bridging $PHCy_2$ Ligand

Piero Leoni*

Scuola Normale Superiore, Piazza dei Cavalieri 7, I-56100 Pisa, Italy

Marco Pasquali* and Milena Sommovigo

Department of Chemistry, University of Pisa, Via Risorgimento 35, I-56126 Pisa, Italy

Alberto Albinati* and Francesca Lianza

Chemical Pharmacy, University of Milan, I-20131 Milan, Italy

Paul S. Pregosin* and Heinz Rüegger

Inorganic Chemistry, ETH-Zentrum, CH-8092 Zürich, Switzerland

Received May 4, 1994[⊗]

The preparation of several new Pd(I) cationic dinuclear complexes containing bridging PCy_2 or PBu^t_2 ligands and terminal phosphine ligands is described. One of these, $[Pd_2(\mu\text{-}PCy_2)(\mu\text{-}PHCy_2)(PEtCy_2)_2]^+$ (**7**), contains a Pd–H–P bridging unit, a relatively rare type of bonding. The cationic complexes $[Pd_2(\mu\text{-}PBu^t_2)(PHCy_2)_4]^+$ (**5**) and $[Pd_2(\mu\text{-}PBu^t_2)(PMe_3)_4]^+$ (**8**) have been isolated and characterized via ^{31}P NMR and X-ray crystallographic studies. The structures reveal large distortions presumably of steric origin. Relevant crystallographic parameters for the two complexes are as follows: for [**5**]BF_4, $C_{56}H_{110}BF_4P_5Pd_2$, monoclinic, space group $P2_1/c$, with a = 20.929(5) Å, b = 15.244(5) Å, c = 20.860(6) Å, β = 75.01(2)°, V = 6429(2) Å^3; for [**8**]CF_3SO_3, $C_{21}H_{54}F_3O_3P_5Pd_2S$, monoclinic, space group $C2/c$, with a = 29.810(3) Å, b = 11.181(1) Å, c = 23.126(4) Å, β = 105.99(9)°, Z = 8, V = 7410(1) Å^3.

Introduction

The chemistry of molecules containing metal–metal bonds continues to be of interest.[1] The presence of an adjacent second metal can help to stabilize a variety of bonding modes. In the chemistry of dinuclear Pd(I) complexes one finds examples of bidentate organometallic ligands which can "chelate" to both metal centers, thereby contributing to the stability of the new complex.[2]

We have recently described the preparation of the Pd(I) dinuclear complex **1** in which there is a novel Pd–H–P bonding mode.[3] The "bridged" secondary phosphine makes use of both metals and is also a good leaving group, thereby allowing preparative access[4] to a series of new cationic complexes arising from **1**, e.g. **2**–**4**. These can be made via reaction of **1** with CO, isoprene, and ethylene, respectively, with the last complex resulting from room-temperature insertion of C_2H_4 into the secondary phosphine P–H bonds. The CO complex **2** crystallizes with the structure shown but exists in solution as a mixture of isomers, with the major geometric isomer having the two secondary phosphines on two separate Pd atoms, but in pseudo-cis positions.[4]

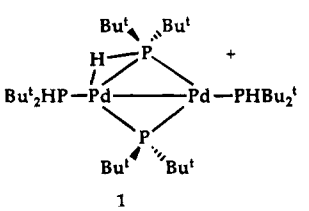

1

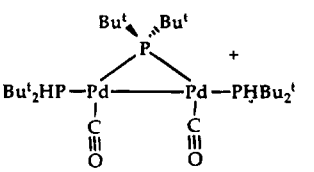

2

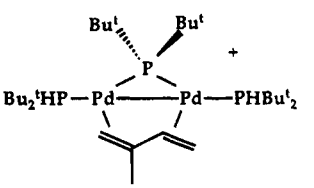

3

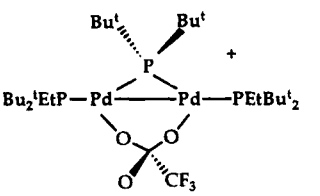

4

[⊗] Abstract published in *Advance ACS Abstracts,* September 1, 1994.

(1) Lewis, J. *Chem. Br.* **1988**, 795. King, R. B. *Inorg. Chim. Acta* **1986**, *116*, 99. Mingos, D. M. P. *Acc. Chem. Res.* **1984**, *17*, 311.

(2) Werner, H.; Kuhn, A. *Angew. Chem., Int. Ed. Engl.* **1977**, *16*, 412. Wilson, W. L.; Nelson, J. H.; Alcock, N. W. *Organometallics* **1990**, *9*, 1699.

(3) Albinati, A.; Lianza, F.; Pasquali, M.; Sommovigo, M.; Leoni, P.; Pregosin, P. S.; Ruegger, H. *Inorg. Chem.* **1991**, *30*, 4690. Leoni, P.; Pasquali, M.; Sommovigo, M.; Laschi, F.; Zanello, P.; Albinati, A.; Lianza, F.; Pregosin, P. S.; Rüegger, H. *Organometallics* **1993**, *12*, 1702.

(4) Leoni, P.; Pasquali, M.; Sommovigo, M.; Albinati, A.; Lianza, F.; Pregosin, P. S.; Rüegger, H. *Organometallics* **1993**, *12*, 4503.

0276-7333/94/2313-4017$04.50/0

It was not clear as to whether **1** exists solely as a consequence of the steric bulk of the Bu^t group. Further, if one wishes to prepare a wide variety of related dinuclear Pd(I) complexes, it would be useful to enhance our understanding of the chemistry of **1** by subjecting it to reactions with, for example, different phosphines. To these ends we have extended our studies and report here on the preparative and stuctural chemistry for several new compounds.

Results and Discussion

Preparative Studies. Reaction of **1** with a 6-fold excess of $PHCy_2$ at room temperature for 2 h afforded complex **5**, which contains the bridging μ-PBu^t_2 and not the bridging PCy_2 ligand, in ca. 85% yield. Prolonged

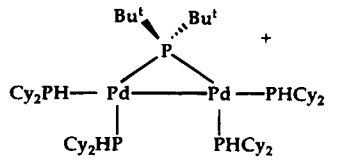

5

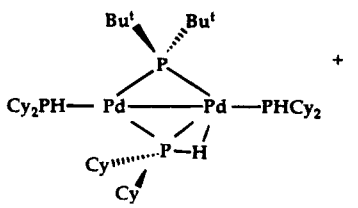

6

reaction times[5] afford $[Pd_2(\mu\text{-}PCy_2)(PHCy_2)_4]^+$, the μ-PCy_2 analog of **5**. Complex **2** is also an acceptable starting material from which **5** can be obtained in high yield. Obviously, the terminal $PHBu^t_2$ ligands readily exchange in the presence of an excess of $PHCy_2$, and cation **5** was prepared as both the triflate and tetrafluoroborate salts. Although this cationic mixed-phosphine complex is stable in the solid state (see below), in solution it is observed to be dynamic on the NMR time scale and exists in equilibrium with **6** and at least one other component.

Reaction of **5** with excess ethylene over a 3-day period gave a 63% yield of **7**, and this represents only the second isolated example of this type of complex. We

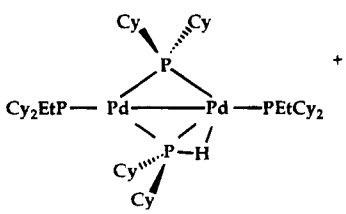

7

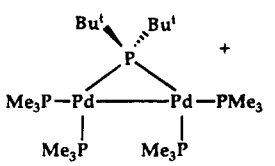

8

have described this type of insertion previously[4] starting from **1**, where the product was **4**. In **7** it is interesting that (a) μ-PBu^t_2 has been exchanged by μ-PCy_2 without addition of further $PHCy_2$ so that **7** must be the thermodynamically more stable cation and (b) whereas **7** contains a bridging μ-$PHCy_2$, a related reaction starting from ethylene and **1** with a μ-PBu^t_2 ligand gave the triflate-coordinated compound **4**.

(5) Pasquali, M., unpublished results.

Scheme 1

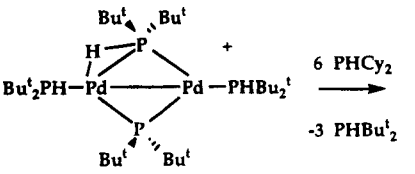

1, as either $CF_3SO_3^-$ or BF_4^- salts

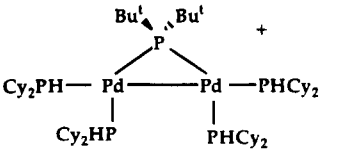

5

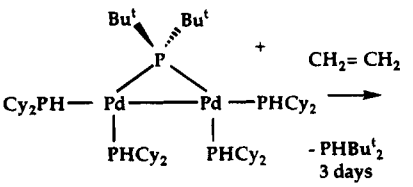

5

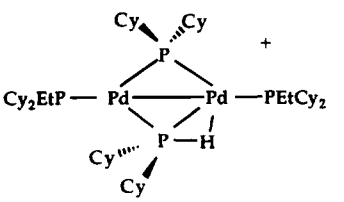

7, as $CF_3SO_3^-$ salt

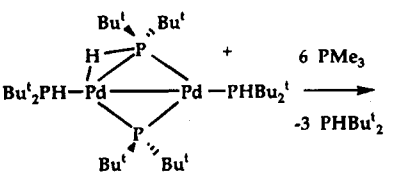

1

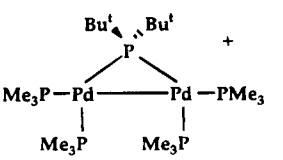

8, as $CF_3SO_3^-$ salt

Complex **8** was obtained from **1** and a 6-fold excess of PMe_3 in 81% yield. This compound could be characterized in both the solid and solution states, although it also shows dynamic behavior on the NMR time scale at ambient probe temperature. Scheme 1 shows a summary of the preparative chemistry.

The ease with which one can substitute the μ-PHR_2 (and μ-PBu^t_2) ligands as well as the terminal secondary phosphines suggests a rich plannable preparative chemistry of Pd(I).

NMR Studies. It is convenient to begin this discussion with complex **8**. The 202 MHz ^{31}P NMR spectrum of this compound in $CDCl_3$ at ambient temperature shows broad signals. These sharpen at 253 K to afford

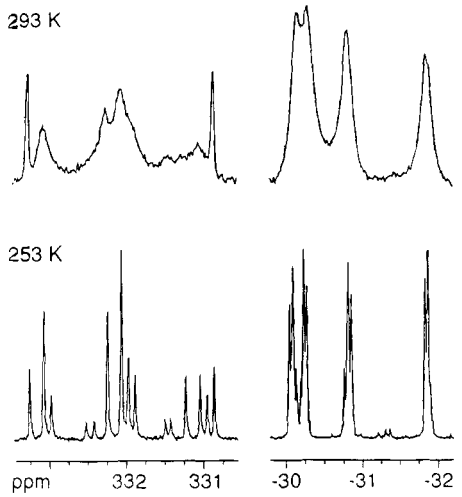

Figure 1. 202 MHz ^{31}P NMR spectra of **8** at 293 K (top) and 253 K (bottom). Note the higher order character of the the high-frequency bridging PBu^t_2 resonance at 253 K as well as the sharp outer lines for this resonance at 253 K.

a surprisingly complicated spectrum (see Figure 1). One can recognize three groups of signals: one arising from the high-frequency μ_2-PBu^t_2 absorption[6] and two due to different types of terminal PMe_3 ligands (δ −30.2 and −31.3). The PMe_3 resonances at δ −31.3 shows a fairly large, ca. 210 Hz $^2J(^{31}P,^{31}P)$ coupling due to its pseudo-trans orientation with respect to the bridging ^{31}P spin, thereby allowing the assignment in this part of the spectrum. The high-frequency bridging PBu^t_2 region, centered around 332.1 ppm, is not symmetric and reveals 15 signals. Simulation of this region clearly shows that this absorption is best considered as the C part of an AA'BB'C spin system, despite the more than 360 ppm difference between the two regions of this ^{31}P spectrum.

The two-dimensional ^{31}P exchange spectrum[7,8] for the PMe_3 section of **8** at 253 K is shown in Figure 2. There are two different types of cross-peaks in this spectrum. The first kind (indicated in the upper spectrum) arises from spin exchange of the bridging PBu^t_2 ligand. This develops when the relaxation time of the spin in question is short when compared to the mixing time. A short T_1 is not unreasonable, given the substantial chemical shift anisotropy[9] and the 11.7 T magnetic field used for the measurement. The second type of off-diagonal cross-peak indicates that the two terminal PMe_3 groups are in slow exchange, at this temperature. Selective decoupling in the ω_1 direction of the bridging ^{31}P spin (lower spectrum) simplifies both PMe_3 resonances but does not affect the exchange. The fine structure in the exchange cross-peaks and the appearance of the ^{31}P μ-PBu^t_2 signal reveal that the exchange

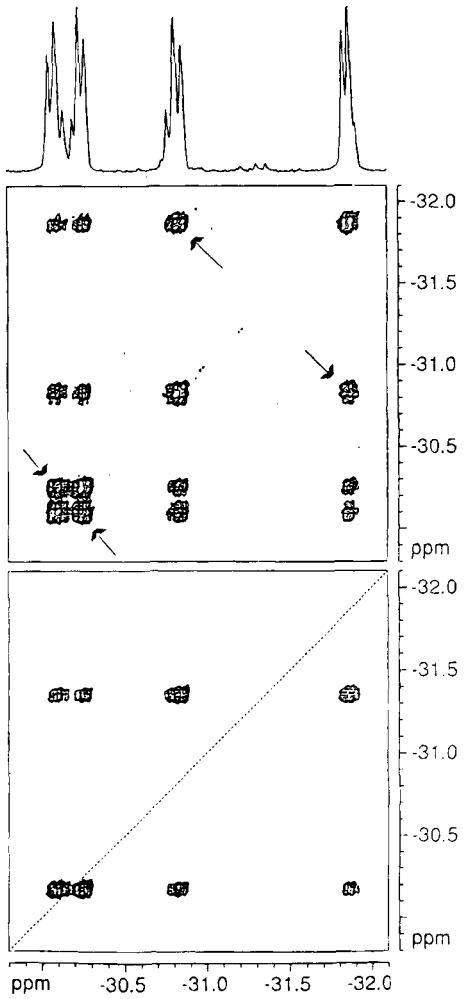

Figure 2. Selective 202 MHz ^{31}P 2-D exchange spectrum for **8**. The bottom trace differs from that of the top in that the bridging ^{31}P spin has been selectively inverted in the middle of the evolution period. There are two types of cross-peaks: those arising from spin exchange (indicated) and those arising from intramolecular PMe_3 exchange.

takes place *with retention of spin configuration*; i.e., it proceeds intramolecularly without PMe_3 dissociation. Further, the observation that the outer lines of the multiplet due to μ-PBu^t_2 are unaffected by the exchange indicates that the signs of the two $^2J(P,P)$ values are the same. One must raise the temperature substantially above room temperature before there are indications of intermolecular exchange. It would seem that, for the complex type $[Pd_2(\mu\text{-}PBu^t_2)(\text{phosphine})_4]^+$, even with four fairly small terminal tertiary phosphine ligands, there is a tendency toward dynamic behavior in solution.

The solid-state 162 MHz ^{31}P CP/MAS spectrum of **8** shows three groups of resonances within a few ppm of their solution chemical shifts. The low-frequency signals are fairly broad and do not show fine structure, whereas the high-frequency resonance shows triplet structure together with the now expected[9] elaborate sideband pattern due to the relatively large chemical shift anisotropy associated with this structural type.

The NMR analysis for **5** was more complicated than for **8**. We begin with the solid-state 162 MHz ^{31}P CP/MAS spectrum of **5**, as it shows the expected five resonances from a single material (we know from the X-ray data that, in the solid, all the ^{31}P spins will be

(6) (a) Powell, J.; Sawyer, J. F.; Stainer, M. V. R. *Inorg. Chem.* **1989**, *28*, 4461. (b) Powell, J.; Sawyer, J. F.; Smith, S. J. *J. Chem. Soc., Chem. Commun.* **1985**, 1312. (c) Powell, J.; Gregg, M. R.; Sawyer, J. F. *J. Chem. Soc., Chem. Commun.* **1987**, 1029.

(7) Hampden-Smith, M. J.; Ruegger, H. *Magn. Reson. Chem.* **1989**, *27*, 1107.

(8) (a) Ruegger, H.; Pregosin, P. S. *Inorg. Chem.* **1987**, *26*, 2912. (b) Ammann, C.; Pregosin, P. S.; Scrivanti, A. *Inorg. Chim. Acta* **1989**, *155*, 217. (c) Ammann, C.; Pregosin, P. S. *Pure Appl. Chem.* **1989**, *61*, 1771.

(9) Power, W. P.; Lumsden, M. D.; Wasylishen, R. E. *Inorg. Chem.* **1991**, *30*, 2997. Power, W. P.; Wasylishen, R. E. *Inorg. Chem.* **1992**, *31*, 2176. Lindner, E.; Fawzi, R.; Mayer, H. A.; Eichele, K.; Hiller, W. *Organometallics* **1992**, *11*, 1033.

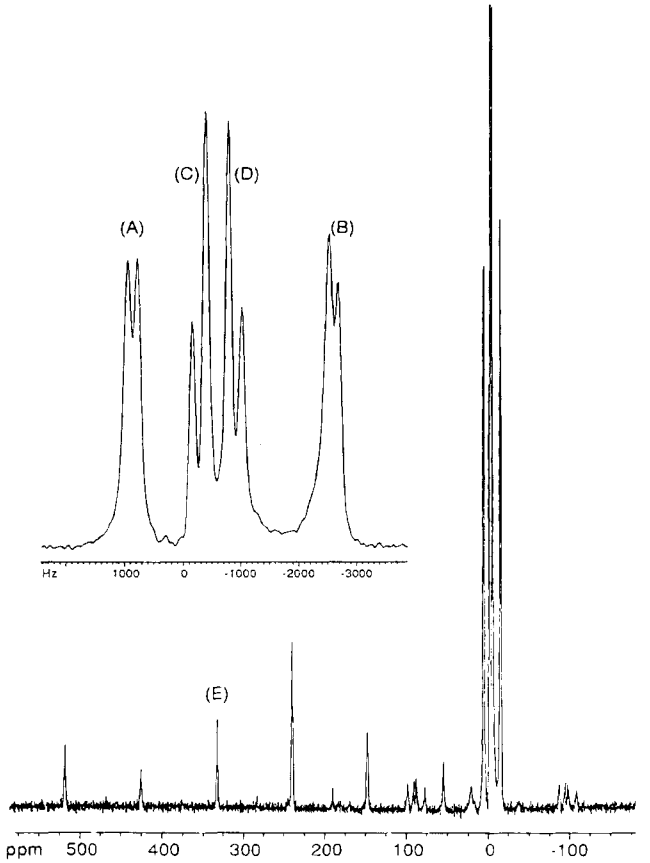

Figure 3. The solid-state 162 MHz ^{31}P CP/MAS spectrum of **5**. The expansion shows the $PHCy_2$ region. The groups of lines marked A and B stem from the ^{31}P spin in a pseudo-trans position to the bridging ^{31}P spin, whereas the groups of lines C and D arise due to nonequivalence of the two $PHCy_2$ ligands in a pseudo-cis position to the bridging ^{31}P spin in the solid state.

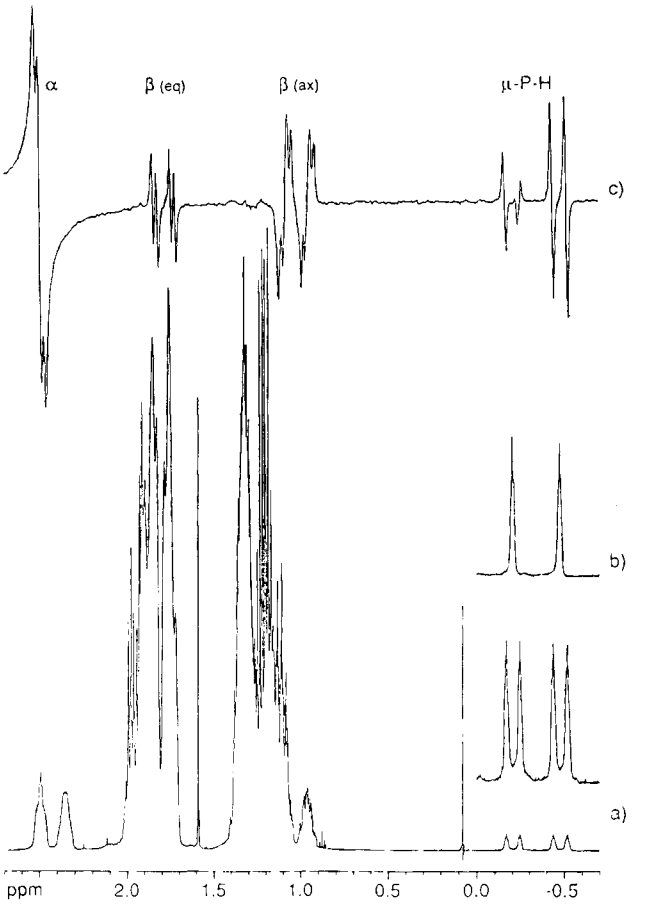

Figure 4. ^1H NMR spectra for **7**: (a) normal 1-D trace showing the bridging $PHCy_2$ proton at relatively high field; (b) the same bridging $PHCy_2$ proton with ^{31}P decoupling at the highest frequency ^{31}P signal (δ 392.3); (c) 1-D COSY experiment with selective excitation at the α-PCH cyclohexyl proton. The β-axial and β-equatorial cyclohexyl protons and the bridging PH are all coupled to the α-PCH.

unique). The bridging PBu^t_2 ligand is a triplet and again shows a complicated sideband pattern centered at ca. 330 ppm. The low-frequency $PHCy_2$ region for **5** (see Figure 3 with its expansion) shows considerable fine structure, resulting mostly from the relatively large trans spin–spin couplings. Basically, the solid-state spectrum is as expected.

In contrast to the solid-state spectrum, the ambient-temperature solution ^{31}P NMR of **5** is moderately complicated and can be interpreted as showing at least three, perhaps four, species. In the high-frequency region the major component shows a broad triplet ($^2J(^{31}P,^{31}P)_{trans}$ = 172 Hz) whose chemical shift, ca. 332 ppm, is in good agreement with the value found for **5** in the solid. In the high-frequency region of the second most abundant component, there are two groups of multiplets centered around ca. 458 and 187 ppm. The corresponding absorptions for **1**, which contains a bridging $PHBu^t_2$ ligand, appear at 455.3 and 217.2, so that we believe this second component to be **6**. The remaining high-frequency signals (ca. 387 and 182 ppm) are weak. The terminal $PHCy_2$ region shows many different resonances, some of which are very broad. At 253 K the ca. 332 ppm signal for **5** dominates the high-frequency section, with those for **6** barely visible. Although lowering the temperature has shifted the equilibrium in favor of **5**, the signals in the $PHCy_2$ region are still broad and unresolved. We interpret the solution data for **5** to mean that it maintains its structure in solution. Presumably, for **5** (and perhaps, at a higher temperature, for **8**) the molecule chooses to dissociate one phosphine to form an intermediate, which due to the presence of secondary phosphines in **5** can be temporarily stabilized as **6**, the $PHCy_2$ analog of **1**.

The procedure for the solution characterization of the new Pd–H–P bridging unit in **1** has been detailed previously.[3] As with **1**, complex **7** shows a bridging proton, just above TMS at δ −0.35, as an apparent doublet of doublets ($^2J(^{31}P,^1H)$ = 136, 40 Hz) (see Figure 4). These two readily visible spin–spin interactions arise from the two *high-frequency*, bridging, ^{31}P spins at δ 392.3 and 179.6. A selective decoupling experiment (Figure 4b) shows that the larger of the two $J(^{31}P,^1H)$ coupling constants, 136 Hz, comes from the ^{31}P resonance at 179.6 ppm, which, in analogy to **1**, we assign to the μ-$PHCy_2$ ligand. This 136 Hz value represents a substantial decrease from the normal[10] one-bond interaction in a coordinated secondary phosphine, e.g., ca 323 Hz for the two $PHBu^t_2$ ligands in **1**. The analogous reduced value in **1** for the μ-$PHBu^t_2$ ligand is 151 Hz. For the PH protons of the terminal ligands in **5** we find δ 4.71 ($^1J(^{31}P,^1H)$ = 297 Hz) and δ 4.65 ($^1J(^{31}P,^1H)$ =

(10) Bentrude, W. G.; Setzer, W. N. In *Methods in Stereochemical Analysis*; Verkade, J. G., Quin, L. D., Eds.; VCH: New York, **1987**; Vol. 8, p 35.

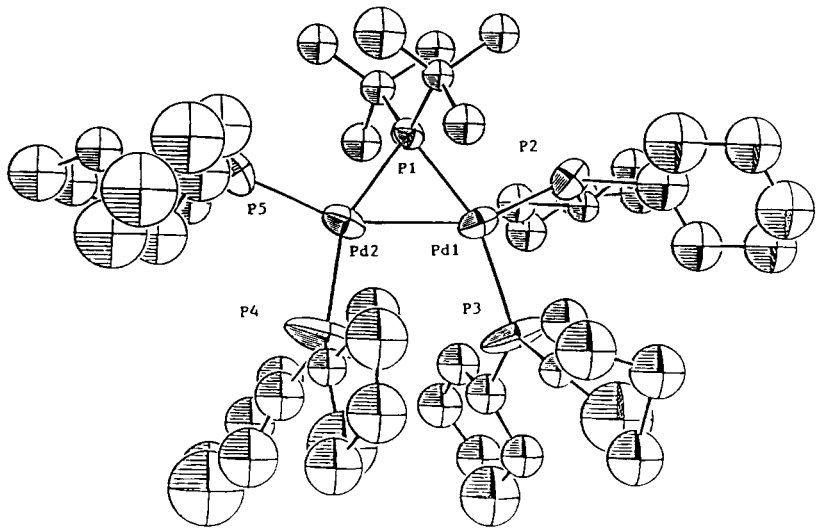

Figure 5. ORTEP plot for the cation **5**.

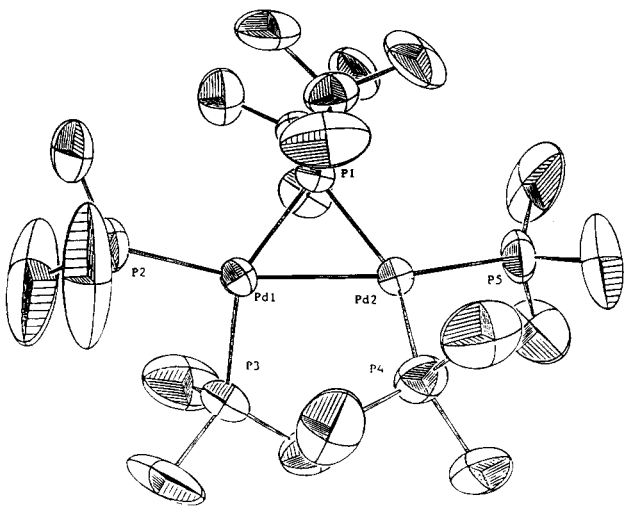

Figure 6. ORTEP plot for the cation **8**. Only one conformation of the terminal phosphines is shown.

309 Hz). There is fine structure on the ^1H lines of the bridging proton which does *not* come from the terminal phosphine ligands but arises from the CH α-protons of the cyclohexyl rings, as shown by the 1-D COSY measurement (Figure 4c). The $P-CH_2CH_3$ proton signals are sharp but not well-resolved, due to overlap with the cyclohexyl protons. The 392.3 ppm ^{31}P chemical shift is as expected[6] for such a bridging μ-PR_2 ligand, as are the positions for the terminal $PEtCy_2$ ligands, 47.0 and 35.1 ppm. It is worth noting that **7** shows the novel Pd—H—P bonding with terminal tertiary phosphines. Up to this point this bonding type had only been observed with terminal secondary phosphine ligands.

X-ray Diffraction Studies. ORTEP views of the cations **5** and **8** are shown in Figures 5 and 6. The immediate coordination sphere in both cations consists of two terminal phosphines, a metal—metal bond, and a bridging PBu^t_2 ligand. The terminal phosphine ligands occupy pseudo-cis and pseudo-trans positions with respect to the bridging ligand. In complex **5** the P atoms of the five ligands and the two Pd atoms lie approximately in one plane with no deviation larger than ±0.1 Å; however, for **8** there are major distortions from planarity as demonstrated by Figure 7. There is

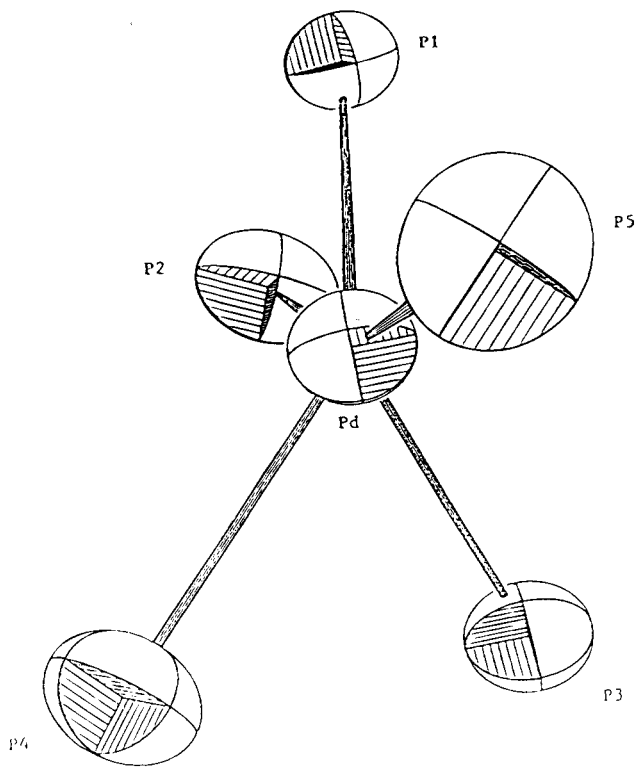

Figure 7. Diagram for **8** based on the X-ray data, showing the positions of the five donor P atoms and the two Pd atoms.

still roughly C_2 symmetry, and this, presumably, explains the poor resolution observed in the solid-state ^{31}P spectrum of this molecule. From Figure 7, it is clear that the structure of **8** is not well represented by the drawing which we have given in the preparative discussion and in the Scheme 1. In fact, the P atoms P(2)—P(5) are +0.64(1), −1.13(1), +1.34(1), and −0.69 Å, respectively, from the plane defined by P(1), Pd(1), and Pd(2). In Table 1 we give a list of selected bond lengths and bond angles for **5** and **8**. We note the following interesting points.

(a) The Pd—Pd bond distance in **5**, at 2.834(4) Å, represents the longest reported Pd—Pd separation in a Pd(I) dinuclear complex. The Pd—Pd bond length in **8**

Table 1. Selected Bond Distances (Å) and Bond Angles (deg) for 5 and 8

	5	8
Pd(1)—Pd(2)	2.834(4)	2.6922(7)
Pd(1)—P(1)	2.262(9)	2.249(2)
Pd(2)—P(1)	2.266(9)	2.253(2)
Pd(1)—P(2)	2.34(1)	2.309(2)
Pd(1)—P(3)	2.35(1)	2.352(2)
Pd(2)—P(4)	2.36(1)	2.350(2)
Pd(2)—P(5)	2.35(1)	2.321(2)
Pd(1)—P(1)—Pd(2)	77.5(2)	73.45(5)
Pd(2)—Pd(1)—P(1)	51.3(2)	53.35(4)
Pd(1)—Pd(2)—P(1)	51.2(2)	53.20(5)
P(1)—Pd(1)—P(2)	105.5(3)	113.3(7)
P(2)—Pd(1)—P(3)	97.0(4)	101.4(1)
Pd(2)—Pd(1)—P(3)	106.3(4)	97.25(6)
P(1)—Pd(1)—P(3)	157.5(5)	140.41(6)
P(1)—Pd(2)—P(5)	104.6(3)	114.20(7)
P(4)—Pd(2)—P(5)	101.0(5)	101.2(1)
Pd(1)—Pd(2)—P(4)	103.5(4)	97.92(6)
P(1)—Pd(2)—P(4)	154.0(5)	136.97(6)
C(111)—P(1)—C(121)	112(1)	110.4(3)
Pd(1)—Pd(2)—P(5)	155.6(3)	159.33(8)
Pd(2)—Pd(1)—P(2)	156.6(2)	159.67(7)

is 2.6922(7) Å and falls in the middle of the known range.[2,6,11-17]

(b) For both **5** and **8**, the Pd—P bond lengths involving the bridging phosphide fall in a narrow range (ca. 2.249–2.266 Å), suggesting little or no difference in this bonding between the two complexes. In the symmetric dimeric complexes $[Pd_2(\mu\text{-}PBu^t_2)_2(PMe_3)_2]$[11] and $[Pd_2(\mu\text{-}PBu^t_2)_2(PHBu^t_2)_2]$[12] the analogous separations are much longer (2.329(3) and 2.336(2) Å, respectively).

(c) The Pd—P terminal phosphine separations are all quite close, with most values close to 2.35 Å, despite the differences between $PHCy_2$ and PMe_3. Relative to **1** or either $[Pd_2(\mu\text{-}PBu^t_2)_2(PMe_3)_2]$ or $[Pd_2(\mu\text{-}PBu^t_2)_2(PHBu^t_2)_2]$ these Pd—P terminal phosphine bond lengths are several hundreths of an angstrom longer.

(d) In **5**, the pseudo-trans angles P(1)—Pd(1)—P(3) (157.5(5)°) and P(1)—Pd(2)—P(4) (154.0(5)°) are considerably larger than the corresponding angles in **8**, (140.41(6) and 136.97(6)°, respectively).

(e) Additional analysis of several of the bond angles in **5** and **8** reveals that both P(2) and P(3) (and also P(4) and P(5)) bend toward the bridging phosphorus atom P(1), presumably to relieve unfavorable steric interactions. Specifically, for **5**, Pd(1)—Pd(2)—P(5) (155.6(3)°) and Pd(2)—Pd(1)—P(2) (156.6(2)°) are both considerably less than the 180° one might have expected. Continuing for **5**, Pd(2)—Pd(1)—P(3) at 106.3(4)° and Pd(1)—Pd(2)—P(4) at 103.5(4)° are both much larger than 90°, again in keeping with a distortion which moves these two terminal $PHCy_2$ ligands away from each other and toward the bridging P atom. The angles Pd(2)—Pd(1)—P(3) at 97.25(6)° and Pd(1)—Pd(2)—P(4) at 97.92(6)° for **8** are not quite so open, possibly because this cation has already twisted some heavy atoms out of the Pd(1), P(1), Pd(2) plane.

We do not know why the structure for **8** is so twisted; however, we note that if **8** had all the heavy atoms in a plane as in **5**, there would be severe steric interactions between the P(3) and P(4) PMe_3 ligands. Given the observed twist, one can imagine that the intramolecular solution dynamics occur via a "continued twist" in which the two PMe_3 ligands, e.g., P(2) and P(3), eventually become perpendicular to the Pd(1), P(1), Pd(2) plane and then relax back with exchange of the ^{31}P spins. In **5**, the cation seems to have found two ways to minimize its energy in that it has lengthened the Pd—Pd bond and arranged two cyclohexyl groups via conformations which reduce their nonbonded interactions. Naturally, we cannot exclude that electronic differences between $PHCy_2$ and PMe_3 may also contribute (pK_a values[18] for these are 4.55 and 8.65, respectively).

Experimental Section

General Considerations. All manipulations were carried out under a nitrogen atmosphere using standard Schlenk techniques. $[Pd_2(\mu\text{-}PBu^t_2)(PHBu^t_2)_2(CO)_2]BF_4$ and $[Pd_2(\mu\text{-}PBu^t_2)(\mu\text{-}PHBu^t_2)(PHBu^t_2)_2]CF_3SO_3$ were prepared as previously described. $PHCy_2$ was purchased from Argus Chemicals and used as received. Solvents were dried by conventional procedures and distilled prior to use. IR spectra (Nujol mull, KBr plates) were recorded on a Perkin-Elmer FT-IR 1725X spectrometer. NMR spectra were measured using Bruker AMX 400 (solid-state) and AMX 500 NMR spectrometers. The ^{31}P exchange spectra were measured by (a) substitution of the three pulses in the normal sequence with a 90° Gauss-shaped soft pulse applied to the region of the terminal phosphine resonances and (b) insertion of an additional 180° Gaussian-shaped soft pulse applied to the region of the bridging phosphide in the middle of the evolution period. The 1-D COSY spectrum was measured as described previously.[19] Solid-state ^{31}P NMR spectra were recorded by employing spinning at the magic angle (with spinning frequencies between 5 and 15 kHz) and cross polarization using contact times between 80 μs and 8 ms.

Preparation of $[Pd_2(\mu\text{-}PBu^t_2)(PCy_2H)_4]CF_3SO_3$ ([5]CF_3SO_3). $PHCy_2$ (0.25 mL, 1.23 mmol) was added to a suspension of $[Pd_2(\mu\text{-}PBu^t_2)(\mu\text{-}PHBu^t_2)(PBu^t_2H)_2]CF_3SO_3$ (184 mg, 0.194 mmol) in dimethoxyethane (DME; 20 mL). The suspension turned from violet to red and the solid started to dissolve. After 2 h the solution was yellow and a yellow solid started to precipitate. The reaction mixture was concentrated to ca. 10 mL, and 25 mL of Et_2O was added. After the mixture was cooled to −30 °C overnight, the solid was filtered and *vacuum* dried (yield 205 mg, 0.157 mmol, 81%). Anal. Calcd for $C_{57}H_{110}F_3O_3P_5Pd_2S$: C, 52.65; H, 8.46. Found: C, 52.92; H, 8.80. IR (Nujol, cm^{-1}): 2314 (w) ν(PH); 1276 (s), 1144 (s), 1032 (vs), 636 (vs) (uncoordinated triflate ion).[20]

Preparation of $[Pd_2(\mu\text{-}PBu^t_2)(PCy_2H)_4]BF_4$ ([5]BF_4). Method a. A procedure similar to the preceding one was utilized by starting from $[Pd_2(\mu\text{-}PBu^t_2)(\mu\text{-}PHBu^t_2)(PBu^t_2H)_2]BF_4$ (195 mg, 0.22 mmol) and $PHCy_2$ (0.27 mL, 1.32 mmol) in DME (20 mL). This afforded 234 mg of the product (0.189 mmol, 86%).

Method b. $PHCy_2$ (0.6 mL, 3 mmol) was added to a solution of $[Pd_2(\mu\text{-}PBu^t_2)(PHBu^t_2)_2(CO)_2]BF_4$ (390 mg, 0.49 mmol) in 20 mL of DME. The orange solution was stirred at room temperature for 2 h. The solvent was then evaporated until a yellow solid started to precipitate. Et_2O was added and, after the mixture was cooled to −30 °C overnight, the solid was

(11) Arif, A. M.; Heaton, D. E.; Jones, R. A.; Nunn, C. M. *Inorg. Chem.* **1987**, *26*, 4228.
(12) Pasquali, M.; Sommovigo, M.; Leoni, P.; Sabatino, P.; Braga, D. *J. Organomet. Chem.* **1992**, *423*, 263.
(13) Budzelaar, P. H. M.; van Leeuwen, P. W. N. M.; Roobeek, C. F. *Organometallics* **1992**, *11*, 23.
(14) Portnoy, M.; Frolow, F.; Milstein, D. *Organometallics* **1991**, *10*, 3960.
(15) Farr, J.; Wood, F. E.; Balch, A. L. *Inorg. Chem.* **1983**, *22*, 3387.
(16) Tanase, T.; Kawahara, K.; Ukaji, H.; Kobayashi, K.; Yamazaki, H.; Yamamoto, Y. *Inorg. Chem.* **1993**, *32*, 3682.
(17) Tanase, T.; Nomura, T.; Fukushima, T.; Yamamoto, Y.; Kobayashi, K. *Inorg. Chem.* **1993**, *32*, 4578.
(18) Streuli, C. A. *Inorg. Chem.* **1962**, *32*, 985.
(19) Emsley, L.; Bodenhausen, G. *J. Magn. Reson.* **1989**, *82*, 211.
(20) Johnstone, D. H. *Inorg. Chem.* **1993**, *32*, 1045.

Table 2. Experimental Data for the X-ray Diffraction Study of [5]BF_4 and [8]CF_3SO_3

	[5]BF_4	[8]CF_3SO_3
formula	$C_{56}H_{110}BF_4P_5Pd_2$	$C_{21}H_{54}F_3O_3P_5Pd_2S$
mol wt	1237.98	811.39
cryst dimens, mm	0.16 × 0.12 × 0.10	0.20 × 0.30 × 0.09
data collecn T, °C	23	23
cryst syst	monoclinic	monoclinic
space group	$P2_1/c$	$C2/c$
a, Å	20.929(5)	29.810(3)
b, Å	15.244(5)	11.181(1)
c, Å	20.860(6)	23.126(4)
β, deg	75.01(2)	105.99(9)
V, Å^3	6429(2)	7410(1)
Z	4	8
ϱ(calcd), g cm^{-3}	1.279	1.455
μ, cm^{-1}	7.170	12.593
radiation	Mo Kα (graphite monochromated, λ = 0.710 69 Å)	
measd reflns	$+h,+k,\pm l$	$\pm h,+k,+l$
θ range, deg	$2.5 < \theta < 23.0$	$2.5 < \theta < 26.0$
scan type	$\omega/2\theta$	$\omega/2\theta$
scan width, deg	1.20 + 0.35 tan θ	1.00 + 0.35 tan θ
max counting time, s	70	90
bkgd time, s	0.5 × (scan time)	0.5 × (scan time)
prescan rejection limit	0.50 (2.00 σ)	0.50 (2.00 σ)
prescan acceptance limit	0.025 (40.00 σ)	0.03 (33.33 σ)
no. of data collected	8858	7035
no. of obsd reflns (n_o)	2784 [$\|F_o\|^2 > 2.5\sigma(\|F\|^2)$]	4074 [$\|F_o\|^2 > 3.5\sigma(\|F\|^2)$]
transmission coeff	0.6165−0.9988	0.9269−0.9967
decay cor		0.9948−1.4416
no. of params refined (n_v)	296	340
fudge factor f	0.060	0.060
max param shift $\Delta p/\sigma$ (at convergence)	<0.4	<0.2
R^a	0.081	0.049
$R_w{}^a$	0.097	0.073
GOF^a	2.923	2.286

^{a} $R = \sum||F_o| - (1/k)|F_c||/\sum|F_o|$. $R_w = [\sum w(|F_o| - (1/k)|F_c|)^2/\sum w|F_o|^2]^{1/2}$, where $w = [\sigma^2(F_o)]^{-1}$ and $\sigma(F_o) = [\sigma^2(F_o^2) + f^2(F_o^2)^2]^{1/2}/2F_o$. GOF = $[\sum w(|F_o| - (1/k)|F_c|)^2/(n_o - n_v)]^{1/2}$.

Table 3. Final Positional and Isotropic Equivalent Displacement Parameters for [5]BF_4[a]

atom	x	y	z	B (Å^2)[b]	atom	x	y	z	B (Å^2)[b]
Pd1	0.7599(1)	0.0248(2)	1.0045(1)	3.91(6)	C323	0.540(2)	−0.130(3)	1.073(2)	10(1)*
Pd2	0.7627(1)	0.0194(2)	0.8680(1)	4.08(6)	C325	0.571(2)	−0.264(3)	1.131(2)	9(1)*
P1	0.7696(4)	0.1374(5)	0.9320(5)	3.1(2)	C326	0.638(4)	−0.220(4)	1.128(3)	16(2)*
P2	0.7698(4)	0.0878(6)	1.1038(5)	4.4(2)	C411	0.664(2)	−0.162(2)	0.843(2)	4.3(7)*
P3	0.7440(5)	−0.1208(6)	1.0432(7)	9.6(4)	C412	0.607(2)	−0.093(2)	0.879(2)	7(1)*
P4	0.7398(5)	−0.1293(7)	0.8503(8)	9.9(4)	C413	0.535(2)	−0.120(3)	0.873(2)	10(1)*
P5	0.7769(5)	0.0769(6)	0.7608(5)	4.9(2)	C414	0.518(2)	−0.206(3)	0.872(2)	9(1)*
C111	0.849(2)	0.203(2)	0.911(2)	3.9(7)*	C415	0.569(2)	−0.274(3)	0.840(2)	9(1)*
C112	0.856(2)	0.259(2)	0.972(2)	5.1(8)*	C416	0.639(3)	−0.256(4)	0.856(3)	13(2)*
C113	0.902(2)	0.131(2)	0.902(2)	5.2(8)*	C421	0.800(2)	−0.208(2)	0.812(2)	7.3(8)*
C114	0.862(2)	0.257(2)	0.849(2)	5.4(9)*	C422	0.868(2)	−0.191(2)	0.818(2)	7(1)*
C121	0.695(1)	0.209(2)	0.950(1)	2.9(6)*	C423	0.927(2)	−0.253(3)	0.794(2)	8(1)*
C122	0.689(2)	0.257(2)	0.891(2)	8(1)*	C424	0.916(3)	−0.314(3)	0.750(2)	10(1)*
C123	0.635(2)	0.144(2)	0.967(2)	4.9(8)*	C425	0.845(4)	−0.332(4)	0.744(4)	18(3)*
C124	0.690(2)	0.267(2)	1.011(2)	4.8(8)*	C426	0.789(3)	−0.286(3)	0.781(3)	11(1)*
C211	0.840(1)	0.054(2)	1.134(1)	3.4(7)*	C511	0.850(1)	0.046(2)	0.699(1)	3.9(7)*
C212	0.904(2)	0.057(2)	1.073(2)	5.4(9)*	C512	0.911(2)	0.040(2)	0.725(2)	6.2(9)*
C213	0.965(2)	0.019(2)	1.097(2)	6.3(9)*	C513	0.975(2)	0.001(2)	0.677(2)	7(1)*
C214	0.976(2)	0.074(2)	1.157(2)	6(1)*	C514	0.986(2)	0.064(2)	0.612(2)	8(1)*
C215	0.913(2)	0.078(2)	1.216(2)	5.9(9)*	C515	0.928(2)	0.073(3)	0.578(2)	10(1)*
C216	0.857(2)	0.111(2)	1.192(2)	5.5(9)*	C516	0.866(2)	0.104(2)	0.634(2)	6.1(9)*
C221	0.702(2)	0.082(3)	1.187(2)	8(1)*	C521	0.712(2)	0.074(3)	0.723(2)	10(1)*
C222	0.694(2)	0.003(2)	1.224(2)	8(1)*	C522	0.706(2)	−0.005(3)	0.684(2)	10(1)*
C223	0.641(2)	0.005(3)	1.289(2)	9(1)*	C523	0.653(3)	−0.006(4)	0.640(3)	13(2)*
C224	0.589(3)	0.052(3)	1.288(2)	11(1)*	C524	0.601(3)	0.046(4)	0.663(3)	14(2)*
C225	0.587(2)	0.133(3)	1.250(2)	10(1)*	C525	0.601(3)	0.109(4)	0.704(3)	13(2)*
C226	0.645(3)	0.135(3)	1.184(3)	12(2)*	C526	0.659(3)	0.128(3)	0.737(2)	11(1)*
C311	0.805(2)	−0.203(2)	1.025(2)	5.4(8)*	C324	0.530(4)	−0.154(5)	1.141(4)	8(2)*
C312	0.875(2)	−0.168(2)	1.007(2)	6(1)*	C324a	0.518(3)	−0.206(4)	1.120(3)	10(1)*
C313	0.933(2)	−0.229(2)	0.997(2)	7(1)*	B	0.769(4)	0.014(5)	0.388(4)	13(2)*
C314	0.921(2)	−0.300(2)	1.040(2)	7(1)*	F1	0.737(3)	0.084(4)	0.351(3)	25(2)*
C315	0.860(3)	−0.346(3)	1.042(3)	13(2)*	F2	0.838(3)	0.006(4)	0.341(3)	38(2)*
C316	0.798(2)	−0.285(2)	1.064(2)	6.1(9)*	F3	0.736(3)	−0.055(3)	0.358(3)	31(2)*
C321	0.663(2)	−0.161(2)	1.072(2)	3.8(7)*	F4	0.772(2)	0.014(3)	0.452(2)	24(2)*
C322	0.611(2)	−0.098(2)	1.067(2)	6.1(9)*					

[a] Estimated standard deviations are given in parentheses. [b] Starred values denote atoms refined isotropically. Anisotropically refined atoms are given in the form of the isotropic equivalent displacement parameter, defined as $^4/_3[a^2\beta_{11} + b^2\beta_{22} + c^2\beta_{33} + ab(\cos\gamma)\beta_{12} + ac(\cos\beta)\beta_{13} + bc(\cos\alpha)\beta_{23}]$.

filtered and *vacuum* dried (yield 531 mg, 0.429 mmol, 87%). Anal. Calcd for $C_{56}H_{110}BF_4P_5Pd_2$: C, 54.3; H, 8.96. Found: C, 53,99; H, 9.18. IR (Nujol, cm^{-1}): 2308 (m), ν(PH); 1054 (vs), ν(BF).

Preparation of [$Pd_2(\mu$-$PCy_2)(\mu$-$PHCy_2)(PEtCy_2)_2$]CF_3SO_3 ([7]CF_3SO_3). [$Pd_2(\mu$-$PBu^t_2)(PHCy_2)_4$]CF_3SO_3 (104 mg, 0.08 mmol) was suspended in DME (20 mL). The reaction flask was evacuated and filled with ethylene. The orange

Table 4. Final Positional and Isotropic Equivalent Displacement Parameters for [8]CF_3SO_3[a]

atom	x	y	z	B (Å^2)[b]
Pd1	0.65136(2)	0.05777(4)	0.61104(2)	3.79(1)
Pd2	0.61772(1)	−0.10886(4)	0.67207(2)	3.75(1)
S	0.61721(8)	−0.5713(2)	0.90854(9)	6.69(5)
P1	0.63847(5)	0.0800(1)	0.70178(7)	3.73(3)
P2	0.65869(9)	0.2378(2)	0.56553(9)	6.84(6)
P3	0.68761(7)	−0.0742(2)	0.55865(8)	5.52(4)
P4	0.56601(7)	−0.2029(2)	0.5893(1)	5.79(5)
P5	0.61406(7)	−0.2370(2)	0.74962(9)	5.86(4)
F1	0.5359(3)	−0.5726(7)	0.8286(3)	11.9(2)*
F2	0.5316(3)	−0.6089(9)	0.9147(4)	16.1(3)*
F3	0.5452(4)	−0.447(1)	0.8959(6)	20.4(4)*
O1	0.6312(2)	0.5606(7)	0.4706(3)	8.9(2)*
O2	0.6314(5)	−0.506(1)	0.8711(7)	18.2(4)*
O3	0.6235(5)	−0.693(2)	0.8928(7)	21.3(5)*
C1	0.5571(4)	−0.565(1)	0.8847(4)	8.6(3)
C111	0.5872(2)	0.1662(7)	0.7140(4)	5.8(2)
C112	0.5487(3)	0.147(1)	0.6541(5)	9.7(3)
C113	0.5973(3)	0.2977(8)	0.7232(4)	8.1(2)
C114	0.5709(3)	0.113(1)	0.7657(4)	9.8(2)
C121	0.6938(2)	0.1196(6)	0.7616(3)	4.9(2)
C122	0.7286(2)	0.0264(8)	0.7566(4)	6.5(2)
C123	0.6875(3)	0.1152(9)	0.8245(4)	7.3(2)
C124	0.7121(3)	0.2426(8)	0.7517(4)	6.9(2)
C211	0.6082(8)	0.250(2)	0.505(1)	21.1(7)
C211a	0.600(1)	0.323(3)	0.550(1)	17.0(9)
C221	0.6570(8)	0.376(1)	0.5974(8)	11.1(5)
C221a	0.694(1)	0.354(4)	0.591(1)	29(1)
C231a	0.653(2)	0.240(2)	0.491(1)	20(1)
C231	0.7151(9)	0.268(3)	0.542(1)	27.8(8)
C311	0.6785(5)	−0.077(1)	0.4775(4)	11.6(3)
C321	0.7493(4)	−0.036(1)	0.5850(6)	11.9(4)
C331	0.6883(3)	−0.2314(8)	0.5754(5)	7.4(2)
C411	0.5074(3)	−0.183(1)	0.5989(6)	10.2(3)
C421	0.5596(4)	−0.138(1)	0.5135(5)	10.6(3)
C431	0.5644(3)	−0.3610(9)	0.5697(5)	9.0(3)
C511	0.6475(5)	−0.369(1)	0.7446(8)	10.8(5)
C511a	0.598(2)	−0.383(3)	0.734(2)	20(2)
C521a	0.577(1)	−0.198(3)	0.805(2)	11.4(9)
C521	0.6379(9)	−0.200(2)	0.8238(7)	16.0(8)
C531a	0.672(1)	−0.253(3)	0.804(2)	12.8(9)
C531	0.5609(5)	−0.303(2)	0.7484(7)	11.6(4)

[a] Estimated standard deviations are given in parentheses. [b] Starred values denote atoms refined isotropically. Anisotropically refined atoms are given in the form of the isotropic equivalent displacement parameter, defined as $^4/_3[a^2\beta_{11} + b^2/\beta_{22} + c^2\beta_{33} + ab(\cos\gamma)\beta_{12} + ac(\cos\beta)\beta_{13} + bc(\cos\alpha)\beta_{23}]$.

suspension was stirred at room temperature for 3 days to give a red solution. The solution was concentrated to ca. 5 mL, and 10 mL of Et_2O was added. After the mixture was cooled to −30 °C overnight, the solid was filtered and *vacuum* dried (yield 61 mg, 0.05 mmol, 63%). Anal. Calcd for $C_{53}H_{99}F_3O_3P_4Pd_2S$: C, 52.6; H, 8.7; P, 10.7. Found: C, 53.6; H, 8.39; P, 10.5. IR (Nujol, cm^{-1}): 1279 (s), 1145 (s), 1032 (vs), 636 (vs) (uncoordinated triflate[20]).

Preparation of $[Pd_2(\mu\text{-}PBu^t_2)(PMe_3)_4]CF_3SO_3$ ([8]CF_3SO_3). $[Pd_2(\mu\text{-}PBu^t_2)(\mu\text{-}PHBu^t_2)(PHBu^t_2)_2]CF_3SO_3$ (439 mg, 0.464 mmol) was suspended in 50 mL of dimethoxyethane. PMe_3 (0.3 mL, 2.9 mmol) was added to the suspension. In a few minutes a red solution formed and a crystalline red solid began to precipitate. Partial evaporation of the solvent and addition of diethyl ether gave 0.304 g (0.375 mmol) of pure $[Pd_2(\mu\text{-}PBu^t_2)(PMe_3)_4]$ CF_3SO_3 (81% yield). Anal. Calcd for $C_{21}H_{54}F_3O_3P_5Pd_2S$: C, 31.1; H, 6.71; P, 19.1. Found, C, 30.6; H, 7.13; P, 18.8.

Crystallography. Crystals suitable for X-ray diffraction of [5]BF_4 and [8]CF_3SO_3 were obtained by crystallization from DME/ether. Crystals of both compounds were mounted on glass fibers (covered for protection with acrylic resin) at a random orientation on an Enraf-Nonius CAD4 diffractometer for the unit cell and space group determinations and for the data collection. Unit cell dimensions were obtained by a least-squares fit of the 2θ values of 25 high-order reflections using the CAD4 centering routines. Selected crystallographic and other relevant data are listed in Table 2.

Data were measured with variable scan speed to ensure constant statistical precision on the collected intensities. Three standard reflections were used to check the stability of the crystal and of the experimental conditions and measured every 1 h. The orientations of the crystals were checked by measuring 3 reflections every 300 measurements. Data have been corrected for Lorentz and polarization factors and for decay ([8]CF_3SO_3) using the data reduction programs of the MOLEN package.[21] Empirical absorption corrections were applied by using azimuthal (ψ) scans of three "high-χ" angle reflections for both sets of data. The standard deviations on intensities were calculated in terms of statistics alone, while those on F_o were calculated as shown in Table 2.

The structures were solved by a combination of Patterson and Fourier methods and refined by full-matrix least squares[21] (the function minimized being $\Sigma[w(F_o - 1/kF_c)^2]$). No extinction correction was found to be necessary. The scattering factors used, corrected for the real and imaginary parts of the anomalous dispersion,[22] were taken from ref 22. All calculations were carried out using the Enraf-Nonius MOLEN package.[21]

Structural Study of [5]BF_4. A total of 8858 independent data were collected, of which only 2784 were observed (cf. Table 2) and used for the refinement. The relevant number of unobserved reflections reflects both the small size of the crystal and the disorder found in the structure, as shown, for example, by the high values of the displacement parameters of some carbon atoms of the phosphine ligands; as a result, the precision of the structure determination is limited.

For the cyclohexyl ring "C321–C326" the Fourier difference maps showed two positions for atom C324 (with occupancy factors, from the refinement, of 0.6 and 0.4 for atoms C324 and C324a, respectively) corresponding to chair and boat conformations. As suggested by the elongated shape of the thermal ellipsoids, atoms P3 and P4 may be disordered. Nonetheless, the refinement of a model including split positions for these two atoms did not give a satisfactory result. Moreover, the BF_4 counterion is also disordered; an idealized model was therefore constructed, based on the strongest peaks found on the Fourier difference map, but refined without constraints.

Given the limited number of observed reflections, only the Pd and P atoms were refined anisotropically. The contribution of the hydrogen atoms in calculated positions (C–H = 0.95 (Å), $B(H) = 1.3B(C_{bounded})$ (Å^2)) was taken into account but not refined. Final atomic coordinates and isotropic displacement factors are given in Table 3.

Structural Study of [8]CF_3SO_3. This structure is also disordered. In particular, the methyl groups bound to atoms P2 and P5 are in two different orientations. The carbon atoms of the two conformations have been refined using both isotropic and anisotropic displacement parameters; while the resulting geometries were comparable, the latter model gave an improved fit as judged from the Hamilton test.[23] The same criterion was used to decide the best model for the refinement of the counterion: anisotropic displacement parameters for the C and S atoms were used, while the F and O atoms were treated isotropically. All other atoms were refined anisotropically. The contribution of the hydrogen atoms, in idealized positions, was taken into account but not refined. Final atomic coordinates and isotropic displacement factors are given in Table 4.

Acknowledgment. P.S.P. thanks the Swiss National Science Foundation and the ETHZ for support and Johnson Matthey, Reading, England, for the loan of palladium salts. A.A. thanks MURST for support.

Supplementary Material Available: For [5]BF_4 and [8]CF_3SO_3, calculated and positional parameters for the hydrogen atoms (Tables S1 and S4), anisotropic displacement parameters (Tables S2 and S5), and additional bond distances and bond angles (Tables S3 and S6) and full numbering schemes (Figures SF1 and SF2) (30 pages). Ordering information is given on any current masthead page.

OM940344W

(21) MOLEN: Molecular Structure Solution Procedure; Enraf-Nonius, Delft, The Netherlands, 1990.
(22) *International Tables for X-ray Crystallography*; Kynoch: Birmingham, England, 1974; Vol. IV.
(23) Hamilton, W. C. *Acta Crystallogr.* **1965**, *13*, 502.